Electronic Supplementary Material (ESI) for Chemical Communications

Supporting Information

Reactivity of an NAD^+ model ligand toward CO_2 reduction in a *fac*-Re(α–diimine)$(CO)_3$Cl complex

Yasuo Matsubara,*[a,b] Sean E. Hightower,[a,c] Jinzhu Chen,[a,d] David C. Grills,[a] Dmitry E. Polyansky,[a] James T. Muckerman,[a] Koji Tanaka,[e] and Etsuko Fujita*[a]

[a] *Brookhaven National Laboratory, Chemistry Department, Upton, New York 11973, USA. Fax: +1-631-344-5815; Tel: +1-631-344-4356; E-mail: fujita@bnl.gov*

[b] *PRESTO, Japan Science and Technology, 4-1-8 Honcho, Kawaguchi-shi, Saitama 332-0012, Japan*

[c] *Current address: Department of Chemistry, University of North Dakota, P.O. Box 9024, Grand Forks, ND 58202-9024, USA*

[d] *Current address: Guangzhou Institute of Energy Conversion, Chinese Academy of Sciences, Guangzhou 510640, P. R. China*

[e] *Institute for Integrated Cell-Material Sciences, Kyoto University, Advanced Chemical Technology Center in Kyoto (ACT Kyoto), Jibuchou 105, Fushimiku, Kyoto 612-8374, Japan*

Experimental section

General Procedures. UV-vis spectra were measured on a Hewlett-Packard 8452A diode-array spectrophotometer. NMR spectra were measured on a Bruker Avance 400 MHz spectrometer. Electrochemical measurements of redox reactions were conducted with a BAS 100B electrochemical analyzer from Bioanalytical Systems. A glassy carbon electrode was used as the working electrode. Emission spectra were measured on a PTI spectrofluorometer. The quantum yield of the emission was determined by comparison with emission from $[Ru(bpy)_3]^{2+}$ in degassed acetonitrile (Φ_{em} = 0.095).[1] The gaseous reaction products, i.e., CO and H_2, were analyzed using GC-FID and -TCD (Agilent Technologies 6890N), respectively, with an active carbon column.

Materials. CH_3CN, CD_3CN, and triethylamine (TEA) were purified in the published manner[2] and vacuum-distilled before use. The 2-(2-pyridyl)-benzo[b]-1,5-naphthyridine (pbn) ligand was prepared from 3-aminoquinoline by a seven-step synthesis using previously reported methods.[3] Other chemicals obtained

from commercial sources were used without purification.

***fac*-[Re(pbn)(CO)$_3$Cl].** A 15 mL toluene solution containing Re(CO)$_5$Cl (11 mg, 30 μmol) and pbn (7.5 mg, 29 μmol) was refluxed for 3 hours under an Ar atmosphere in the dark. The precipitated brownish solid was filtered, washed with hexane and dried under vacuum. If necessary, column chromatography using neutral aluminum oxide (Brockmann activity: I) and dichloromethane containing methanol (0 – 0.4 v%) as eluent was used for purification of the crude product. The first orange band was collected and the eluent was evaporated. The resulting solid was then recrystallized from THF/hexane. Yield: 7 mg, 43%. Anal. Calcd for $C_{20}H_{11}ClN_3O_3Re$: C, 42.67%; H, 1.97%; N, 7.46%. Found: C, 42.94%; H, 2.07%; N, 7.19%. ^{1}H-NMR (400 MHz, CD$_3$CN): δ 9.86 (s, 1H, 10), 9.26 (ddd, *J* = 5.4, 1.4, 0.8 Hz, 1H, py-6), 8.95 (dd, *J* = 9.3, 0.9 Hz, 1H, 3), 8.76 (d, *J* = 9.3 Hz, 1H, 4), 8.71 (d, *J* = 8.2 Hz, 1H, py-3), 8.36 (d, *J* = 8.5 Hz, 1H, 9), 8.33 (ddd, *J* = 8.2, 7.8, 1.4 Hz, 1H, py-4), 8.31 (d, *J* = 8.8, 0.8 Hz, 1H, 6), 8.04 (ddd, *J* = 8.8, 6.7, 1.4 Hz, 1H, 7), 7.82 (ddd, *J* = 8.5, 6.7, 0.8 Hz, 1H, 8), 7.77 (ddd, *J* = 7.8, 5.4, 1.2 Hz, 1H, py-5). ν(CO): 2023, 1921 and 1903 cm^{-1}. ESI-MS: *m/z* = 585.9, calc: 586.0 for [M + Na$^+$]$^+$.

Photoreduction of *fac*-[Re(pbn)(CO)$_3$Cl]. 5 mL of a 5% (v/v) TEA/CH$_3$CN solution containing *fac*-[Re(pbn)(CO)$_3$Cl] (0.3 mg, 0.5 μmol) was prepared. 4 mL of the stock solution was placed into a flask equipped with a quartz cuvette (*d* = 1 cm) and a drop of water (H$_2$O or D$_2$O) was added to the flask under an Ar atmosphere in the absence of direct light. The solution was degassed by three freeze-pump-thaw cycles and then irradiated with a 150-W Xenon lamp equipped with a water filter and a 420-nm LP filter. After no more changes in the UV-vis absorption spectrum were observed (about 1 min), the solvent was removed under a reduced pressure (< 10^{-6} Torr). The orange-yellow solid product was then taken up in 0.55 mL of dry CD$_3$CN and passed through a 0.2 μm inorganic membrane filter (Whatman) into a 5-mm J-Young style NMR tube. For measurement of quantum yield, a 75-W Xenon lamp was used with a water filter and a monochromater (436 ± 8 nm) and the incident light intensity into the solution in a quartz cuvette (*d* = 1 cm) was determined to be (1.1 ± 0.1) × 10^{-9} einstein s^{-1}, which was determined using a K$_3$Fe(C$_2$O$_4$)$_3$ actinometer.[4]

Reduction of *fac*-[Re(pbn)(CO)$_3$Cl] with Sodium Dithionite. *fac*-[Re(pbn)(CO)$_3$Cl] (0.3 mg, 0.5 μmol) was added to CH$_3$CN (3 mL), and then an aqueous solution of Na$_2$S$_2$O$_4$ (0.2 mL, 5 μmol) was added under an Ar atmosphere. The addition of Na$_2$S$_2$O$_4$ to the solution caused an immediate change of the solution color from red-orange to orange, followed shortly afterwards to a bright yellow color (~ 5 min). After the solution was allowed to stir for 4 h, the solvent was removed under a reduced pressure (< 10^{-6} Torr). The orange-yellow solid product was then taken up in 0.55 mL of dry CD$_3$CN and passed through a 0.2 μm inorganic membrane filter (Whatman) into a 5-mm J-Young style NMR tube. Since Na$_2$S$_2$O$_4$ is insoluble in CH$_3$CN, this filtration essentially removed the remaining Na$_2$S$_2$O$_4$ from the solution. ^{1}H NMR (400 MHz, CD$_3$CN): δ 8.94 (d, *J* = 5.6 Hz, 1H, py-6), 8.15 (d, *J* = 8.3 Hz, 1H, py-3), 8.07 (dd, *J* = 8.3, 7.5 Hz, 1H, py-4), 8.03 (d, *J* = 8.9 Hz, 1H, 3-H), 7.78 (s, 1H, -NH), 7.47 (dd, *J* = 7.5, 5.6 Hz, 1H, py-5), 7.30 (d, *J* = 8.9 Hz, 1H, 4-H), 7.18 (d, *J* = 7.5 Hz, 1H, 9-H), 7.15 (dd, *J* = 8.0, 7.5 Hz, 1H, 7-H), 6.94 (dd, *J* = 7.5, 7.5 Hz, 1H, 8-H), 6.81 (d, *J* = 8.0 Hz, 1H, 6-H), 4.84 (d, *J* = 21 Hz, 1H, -CH$_2$), 4.77 (d, *J* = 21 Hz, 1H, -CH$_2$). ESI-MS: *m/z* = 588.1, calc: 588.0 for [M + Na$^+$]$^+$. A similar experiment was carried

out using a D_2O solution of $Na_2S_2O_4$.

Na-Hg reduction of *fac*-[Re(pbn)(CO)$_3$Cl]. A small amount of *fac*-[Re(pbn)(CO)$_3$Cl] (< 0.5 mg) was placed into special glassware equipped with an optical cell. After sodium amalgam (Na-Hg, 0.5% Na in Hg) was placed into a separate compartment separated from the main compartment by a frit, and a certain amount of dry THF was vacuum-transferred to the glassware, the glassware was flame-sealed. Generation of the reduced species was achieved by gradually bringing small amounts of the solution in and out of contact with the amalgam, while monitoring the UV-vis absorption spectral changes.

Electrochemical Measurements. To determine redox potentials, cyclic voltammograms (CVs) were recorded, together with Osteryoung square wave voltammetry (OSWV)[5] using a BAS-100B electrochemical analyzer, in deaerated acetonitrile with *n*-Bu_4NPF_6 (0.1 M) as a supporting electrolyte under argon atmosphere at 295 ± 5 K. A standard three-electrode cell was used, which consisted of a glassy carbon electrode (3 mm in diameter), a platinum wire and Ag/$AgNO_3$ (0.01 M) in *n*-Bu_4NPF_6 (TBAH) acetonitrile solution for the working, counter and reference electrodes, respectively. The effective surface area of the working electrode was determined as 7.1 mm^2 according to a method reported in the literature.[6] The ferrocenium/ferrocene (Fc^+/Fc) redox couple was measured as a secondary standard. In order to determine a value of the current function (χ),[7] the concentration (C_0*) of *fac*-[Re(pbn)(CO)$_3$Cl] in the solution was determined by the absorbance at 382 nm in its UV-vis spectrum and diffusion constants (D_0) of the complex was assumed as 1×10^{-5} cm^2 s^{-1}. For measurement of voltammograms of an acidic solution, a stationary mercury drop, which was prepared by EG&G PARC 303A SMDE, was used as the working electrode and its surface area was about 1 mm^2. The solubility of CO_2 in wet acetonitrile (~0.3 M of water) was used as 260 mM at 297 ± 5 K.[8] A series of CO_2-N_2 mixture gases (100, 30.3, 9.9, 3.0 and 0.1% CO_2 in N_2) were used to regulate the concentration of CO_2 in solution.

Controlled Potential Electrolysis. Bulk electrolysis experiments were carried out with 0.2 mM **Re**(pbn) in an air-tight cell sealed with Teflon-silicone rubber disks in GL14-threaded fittings. The cell was fitted with a glassy carbon working electrode (6 mm in diameter), a platinum coil counter electrode isolated from the solution electrolyzed via a Vycor frit, and a Ag/$AgNO_3$ (0.01 M) reference electrode. Gas phase samples from the cell were analyzed by GC-TCD and -FID. Formic acid produced in the electrolyte solution during electrolysis was quantified by an ion chromatography system (Thermo Scientific Dionex ICS-1600) using a suppressor (Dionex ERS 500) and an anion-exchange column (Dionex IonPac AS23) with an aqueous potassium hydroxide solution (30 mM) as an eluent. The solution was diluted by ten-times with deionized water and filtered just before analysis.

Experimental details of the femtosecond pump-probe experiment. For the ultrafast transient absorption (TA) measurements, 450 nm pump pulses were generated in an optical parametric amplifier (Coherent Opera Solo) that was pumped by the output (3.5 mJ at 1kHz repetition rate) of a Ti:Sapphire-based regenerative amplifier (Coherent Legend Elite). A small part (<5 μJ) of the output of the regenerative amplifier was used to generate the continuum probe used inside of a commercial ultrafast TA spectrometer (Helios, Ultrafast Systems). The repetition rate of the system was 1kHz and the instrument response was determined by the formation time of free carriers in an a-Si:H thin film (<2μm) to be 150fs.

Experimental details of the picosecond transient digitizer experiment. The output of the third harmonic (355 nm) of a picosecond mode-locked Nd:YAG laser (Continuum, Leopard, SS-10-SV, ~ 60 ps pulse width) was overlapped with the output from a pulsed Xe Arc lamp (150 W Newport lamp; Applied Photophysics 150 W power supply and pulser unit) in a 90° beam configuration inside a 1 cm pathlength four-window quartz cuvette. The probe light was passed through a 10 nm bandpass interference filter (Cheshire Optical) and focused into a positively biased (2.5 kV) biplanar tube (Hamamatsu, R1328U-53). The output of the biplanar tube was digitized by a fast oscilloscope (LeCroy, WAVEMASTER 8620A, 6 GHz; 20 GS/s) and the recorded waveforms with and without laser excitation were used to calculate the change in optical density as a function of time.

Photoreduction of *fac*-[Re(pbn)(CO)$_3$Cl]

When **Re**(pbn) (**Re** = ReCl(CO)$_3$) was irradiated using visible light (> 420 nm) in an acetonitrile solution containing triethylamine under an Ar atmosphere, rapid UV-vis absorption spectral changes were observed, which were completed in under 20 s as shown in Figure S1. Well-defined isosbestic points were observed during the progress of the reaction. The ^{1}H-NMR spectrum of the photoproduct (prepared in a 5% (v/v) TEA/CH$_3$CN solution with a drop of H$_2$O) was also identical to that of a product prepared using sodium dithionite in a CH$_3$CN/H$_2$O solution (Figure S2). The peaks in the spectrum were assigned to the two-electron-reduced and doubly protonated complex, i.e., **Re**(pbnHH). All peaks due to **Re**(pbnHH) were shifted upfield compared with the corresponding peaks of **Re**(pbn) and a peak due to protons at the C$_{10}$ position was observed as a typical geminal coupled peak ($^2J_{AB}$ = 21 Hz) at 4.80 ppm caused by non-equivalency of the two sites at the C$_{10}$ position. Its integrated area was two relative to that of the other peaks. This complex was also observed in ESI-MS as [**Re**(pbnHH) + Na$^+$]$^+$ (*m/z* = 588.1, calc: 588.0). Therefore, it was found that quantitative formation of **Re**(pbnHH) takes place during photoirradiation. The quantum yield of this photoreaction was determined as 0.33 upon excitation at 436 ± 8nm.

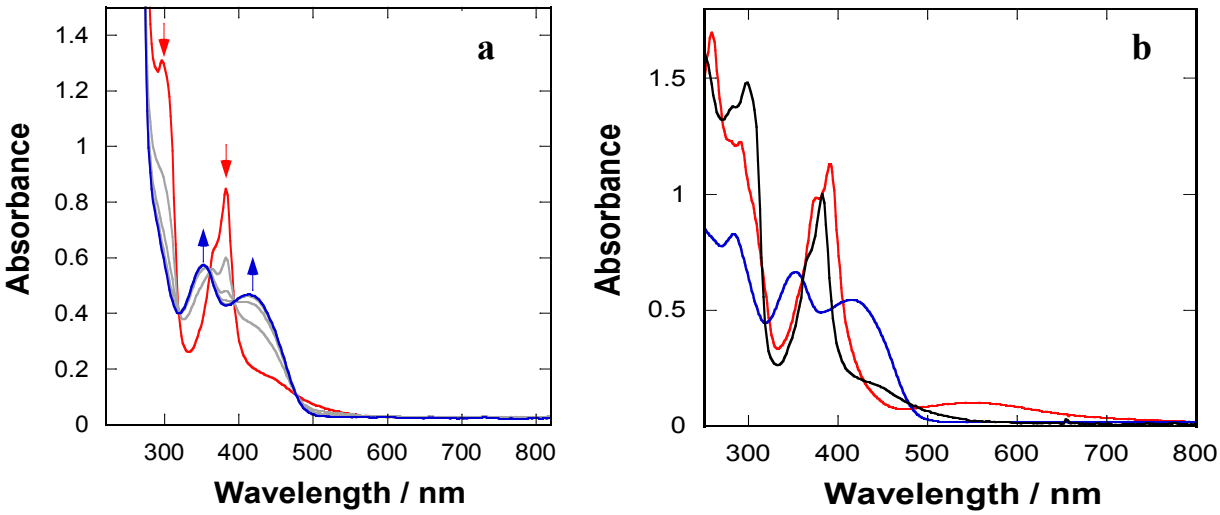

Figure S1. (a) UV-vis absorption spectral changes of **Re**(pbn) (red) to give **Re**(pbnHH) (blue) in a CH$_3$CN solution containing TEA during an irradiation for 20 s recorded at intervals of 5 s. (b) UV-vis absorption spectra of **Re**(pbn) (black) and **Re**(pbnHH) (blue) in acetonitrile and **Re**(pbnH$^+$) (red) in dichloromethane.

When H$_2$O was replaced by D$_2$O in the photochemical reaction, the peak due to protons at the C$_{10}$ position disappeared completely without any changes in other peaks (Figure S3a). This species was assigned to *fac*-[Re{(5,10,10-^{2}H$_3$)2-(pyridin-2-yl)-5,10-dihydrobenzo[b][1,5]naphthyridine}(CO)$_3$Cl], **Re**(C$_{10}$D-pbnDD). In contrast, the peak was observed as two singlets at 4.80 and 4.76 ppm in the ^{1}H-NMR spectrum of a product prepared by sodium dithionite with D$_2$O (Figure S3b). This species was assigned to *fac*-[Re{(5,10-^{2}H$_2$)2-(pyridin-2-yl)-5,10-dihydrobenzo[b][1,5]naphthyridine}(CO)$_3$Cl], **Re**(pbnDD). Note

that the peak of the -NH proton appears due to exchange of deuterons in the NMR-solvent.

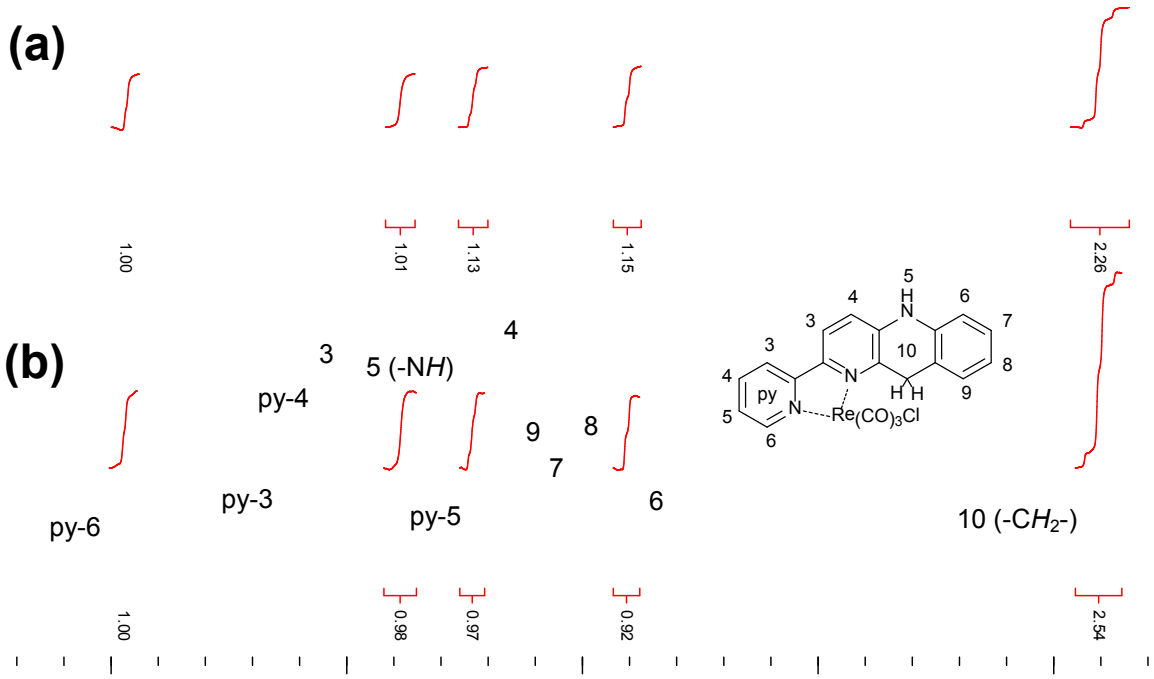

Figure S2. ^{1}H-NMR spectra of a dry CD_3CN solution at 25 °C containing **Re**(pbnHH) acquired by (a) photoreduction and (b) chemical reduction using $Na_2S_2O_4$.

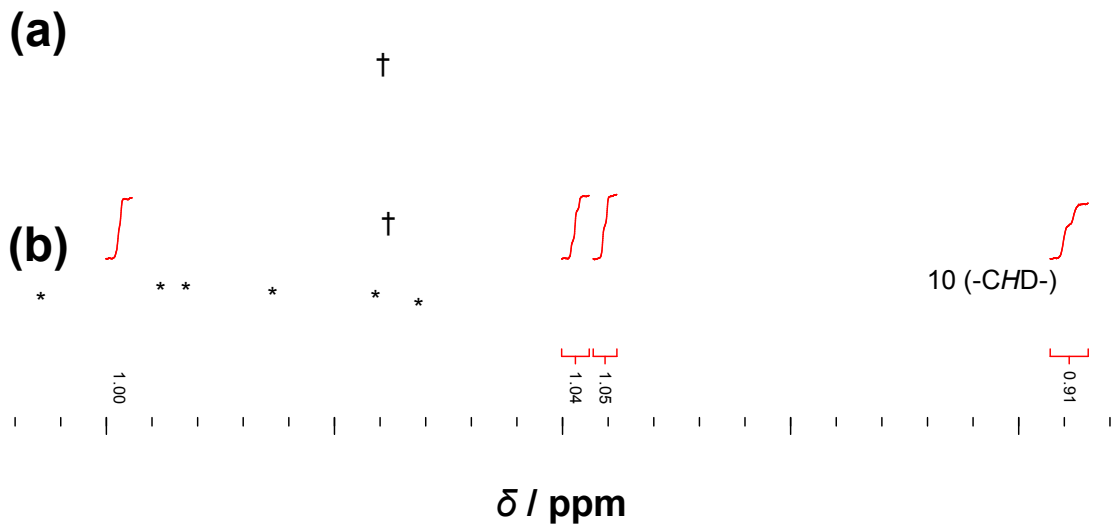

Figure S3. ^{1}H-NMR spectra of a dry CD_3CN solution at 25 °C containing **Re**(C_{10}D-pbnDD) and **Re**(pbnDD) acquired by photoreduction with D_2O (a) and chemical reduction using $Na_2S_2O_4$ with D_2O (b), respectively. The marks († and *) indicate the peak of the -NH proton which appears due to exchange of deuteron in the NMR-solvent and the peaks of unreacted **Re**(pbn), respectively.

In its partial photoreduction with irradiation for only five seconds, the ^{1}H-NMR spectrum of the product consisted mainly of **Re**(C_{10}D-pbnDD) (*ca.* 72%) and mono-deuterated complex *fac*-[Re{(10-^{2}H)2-(pyridin-2-yl)-benzo[b][1,5]naphthyridine}$(CO)_3$Cl], **Re**(C_{10}D-pbn); *ca.* 24%, which was calculated based on the integrated ratio of the peak due to the proton at the C_{10} position of the pbn moiety) as shown in Figure S4 and Scheme S1. The ratio of **Re**(pbnDD) was small (*ca.* 3%, which was estimated based on the integrated ratio of the peak due to the proton at the C_{10} position of the pbnDD moiety). Both **Re**(C_{10}D-pbnDD) and **Re**(C_{10}-pbn) were clearly detected in ESI-MS as [**Re**(C_{10}D-pbnHD) + Na^+]$^+$ (*m/z* = 590.0, calc: 590.0) and [**Re**(C_{10}D-pbn) + Na^+]$^+$ (*m/z* = 587.1, calc: 587.0), respectively (Figure S5). Here [**Re**(C_{10}D-pbnHD) + Na^+]$^+$ is produced during the ESI-MS measurement via an exchange of a deuteron of –ND in **Re**(C_{10}D-pbnDD) for a proton in wet methanol used as the solvent. These deuterium exchange reactions did not take place without TEA and/or irradiation.

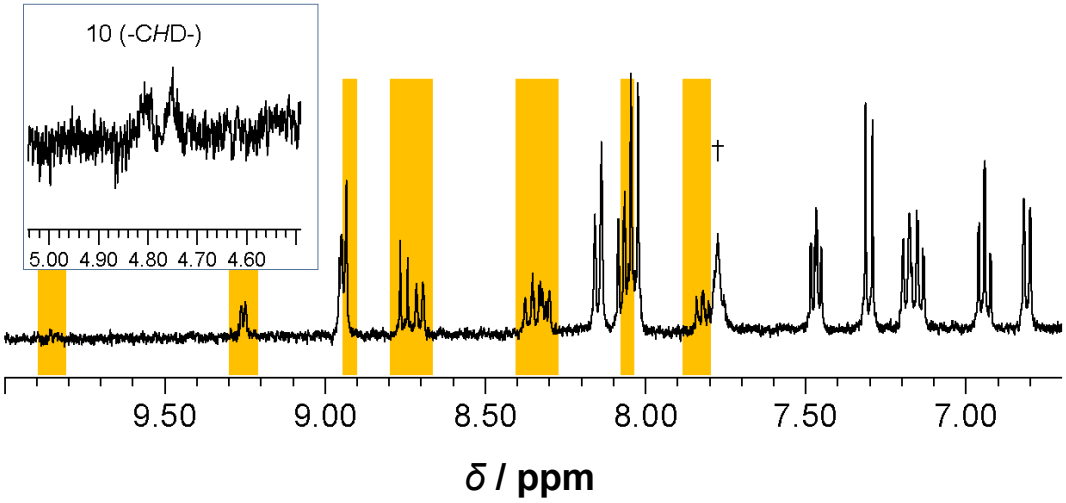

Figure S4. ^{1}H-NMR spectra of a dry CD_3CN solution of photoproducts acquired by the irradiation of **Re**(pbn) in CH_3CN solution containing TEA with a drop of D_2O for only five seconds. The colored peaks are assigned to **Re**(C_{10}D-pbn) or unreacted **Re**(pbn). The mark (†) indicates the peak of the -NH proton which appears due to exchange of deuteron in the NMR-solvent.

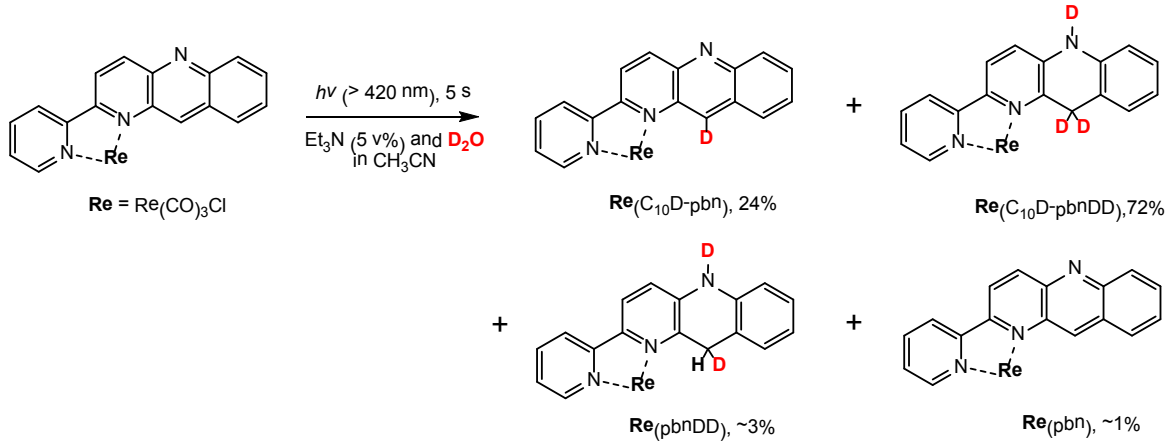

Scheme S1. Photoreaction of Re(pbn) in a CH_3CN solution containing Et_3N and D_2O with 5 s irradiation.

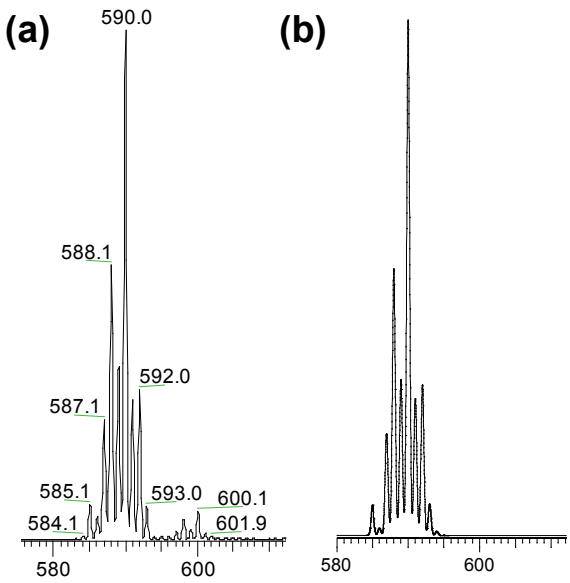

Figure S5. (a) ESI-MS spectrum of a CH_3OH solution of the photoproduct acquired by the irradiation of **Re**(pbn) in CH_3CN solution containing TEA and a drop of D_2O for only five seconds.(b) Its simulated spectrum consisted of [**Re**(C_{10}D-pbnHD) + Na^+]$^+$ and [**Re**(C_{10}D-pbn) + Na^+]$^+$ (4:1). [**Re**(C_{10}D-pbnHD) + Na^+]$^+$ is produced during the ESI-MS measurement via an exchange of a deuteron of –ND in **Re**(C_{10}D-pbnDD) for a proton in wet methanol used as the solvent.

Upon a 20-seconds irradiation of a CH_3CN solution containing Et_3N and a drop of D_2O, **Re**(pbn) converts completely to **Re**(C_{10}D-pbnDD), which is a completely deuterated species at the C_{10} position as shown in Figure S3a. In the case of $Ru(bpy)_2(pbn)^{2+}$, it has been reported that only $Ru(bpy)_2(pbnDD)^{2+}$ is formed stereo-selectively.[9] In contrast, during the partial photoreduction of **Re**(pbn), a deuterated starting

complex, i.e., C_{10}D-pbn and a single deuterated reduced complex, i.e. Re(C_{10}D-pbn) was produced in addition to C_{10}D-pbnDD. While 24% of **Re**(pbn) was converted to Ru(C_{10}D-pbn), only 3% of **Re**(pbnDD) was produced. Since the production of **Re**(C_{10}D-pbnDD) takes place only upon irradiating with Et_3N, it is conceivable that these deuterations take place with the aid of a photoproduced $Et_3N^{\bullet+}$ as shown in Scheme 2. In this reaction, **Re**(pbnDD) is likely produced together with $Et_3N^{\bullet+}$, at first in the same manner as in the case of $Ru(bpy)_2(pbn)^{2+}$. $Et_3N^{\bullet+}$ is known to abstract an H atom from Et_3N. However, the C–H bond at the C_{10} position of the **Re**(pbnDD) will be a much better H-atom donor than the C–H bond in Et_3N (cf. the C–H bond dissociation energy of 77 kcal/mol for 1,4-cyclohexadiene vs. 91 kcal/mol for Et_3N). Therefore, the H-atom at the C_{10} position of **Re**(pbnDD) might be preferentially abstracted by $Et_3N^{\bullet+}$ to give [Re(C_{10}D-pbnD$^{\bullet}$), which is **A** in Scheme S2. **Re**(C_{10}D-pbnDD) and **Re**(C_{10}D-pbn) are then produced by a disproportion reaction between two **Re**(C_{10}D-pbnD$^{\bullet}$) complexes. The reason why these deuterations do not take place in the case of $Ru(bpy)_2(pbn)^{2+}$ is probably due to its greater steric hindrance and charge.

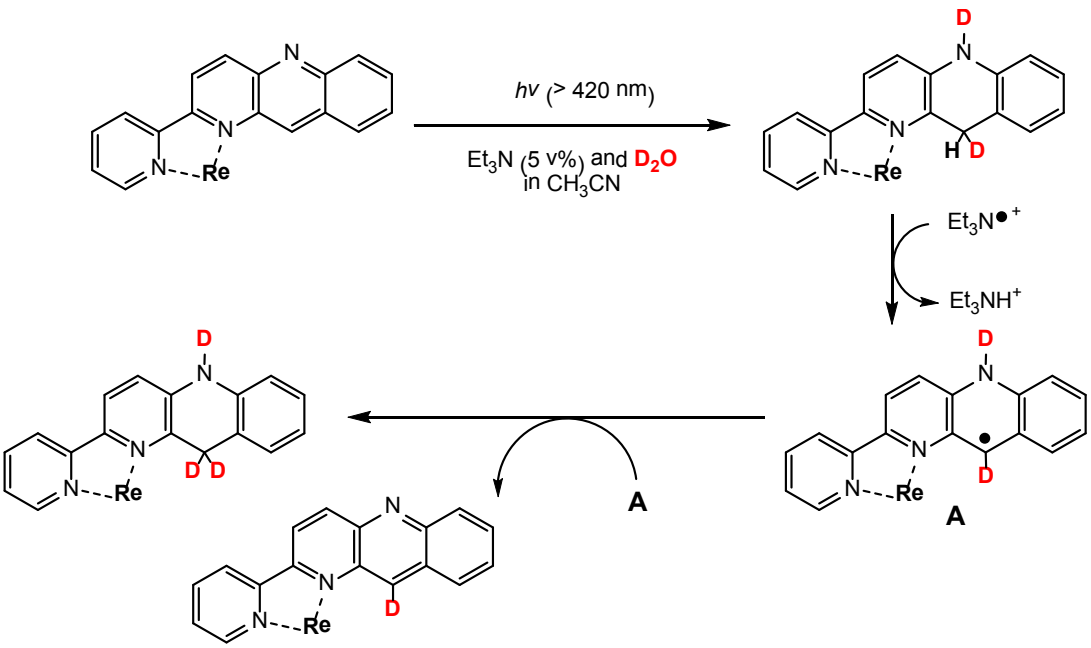

Scheme S2. Proposed mechanism of the deuteration of **Re**(pbnDD) via **A**, to give **Re**(C_{10}D-pbn) and **Re**(C_{10}D-pbnDD). $Et_3N^{\bullet+}$ is a photoproduct.

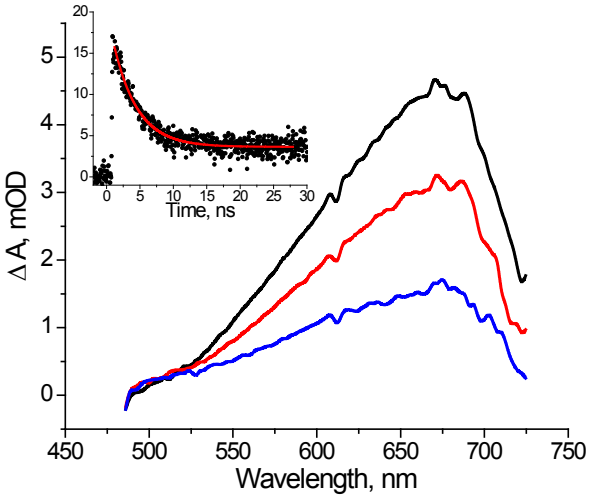

Figure S6. Transient absorption spectra recorded 0.13 ns (black), 0.88 ns (red) and 2.5 ns (blue) after the 450 nm laser excitation pulse during a femtosecond pump-probe experiment on **Re**(pbn) in acetonitrile. The insert shows the decay of the transient absorption at 650 nm, recorded during a picosecond transient digitizer experiment after 355 nm excitation of **Re**(pbn) in acetonitrile.

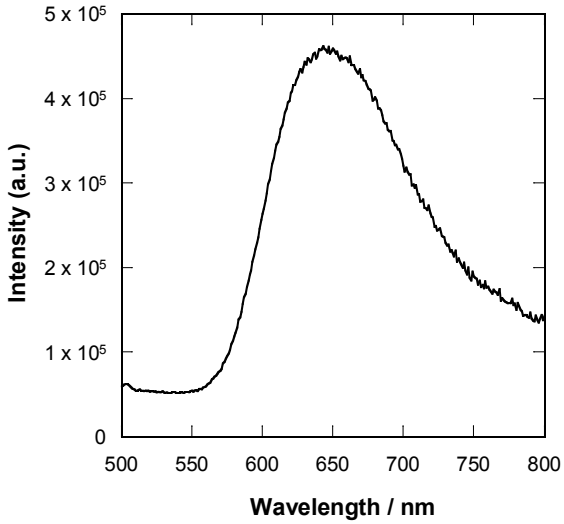

Figure S7. Corrected emission spectrum of **Re**(pbnHH) at 295 K in acetonitrile.

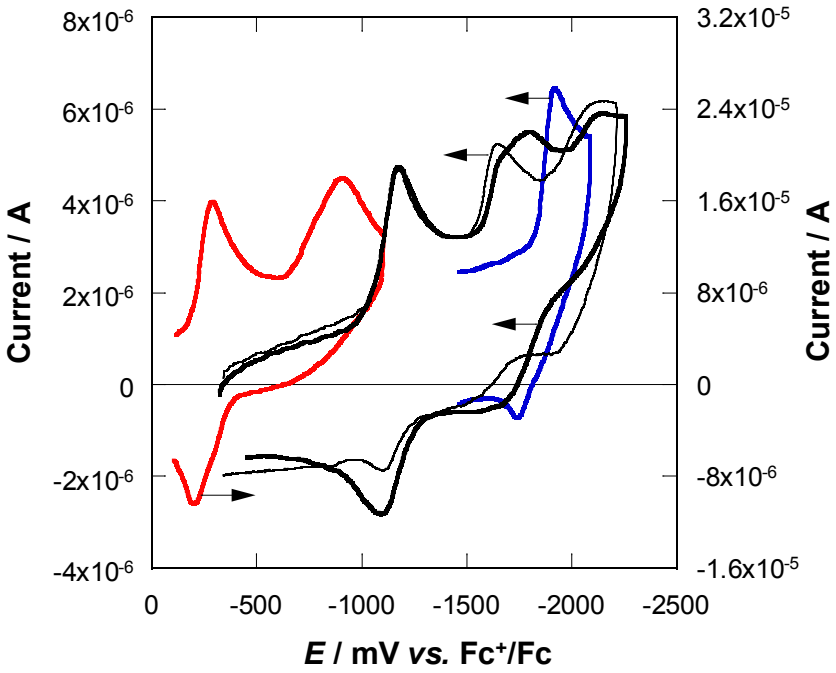

Figure S8. CVs of **Re**(pbn) (black) and **Re**(pbnH$^+$) synthesized *in situ* (red) in dry acetonitrile solutions; and **Re**(pbn) (thin black) and **Re**(pbnHH) (blue) in wet acetonitrile solutions (~0.3 M of water) under an Ar atmosphere. For **Re**(pbn) and **Re**(pbnHH), each voltammogram was taken at scan rates of 100 mV/s in a solution of the compound (0.20 mM) with TBAH (0.1 M) using a glassy carbon working electrode (area = 7.1 mm^2). For [**Re**(pbnH)]$^+$, the voltammogram was taken at a scan rate of 3.2 V/s in a solution of the compound (0.20 mM) with TBAH (0.1 M) and $HBF_4(OEt_2)_2$ (2 mM) using a stationary mercury drop working electrode (area ~ 1 mm^2). A shoulder at –1.65 V (vs Fc$^+$/Fc) is due to the species formed by a trace amount of water in acetonitrile, because the peak at –1.80 V was suppressed by addition of water to the acetonitrile solution and a new peak appeared at –1.65 V (thin black line).

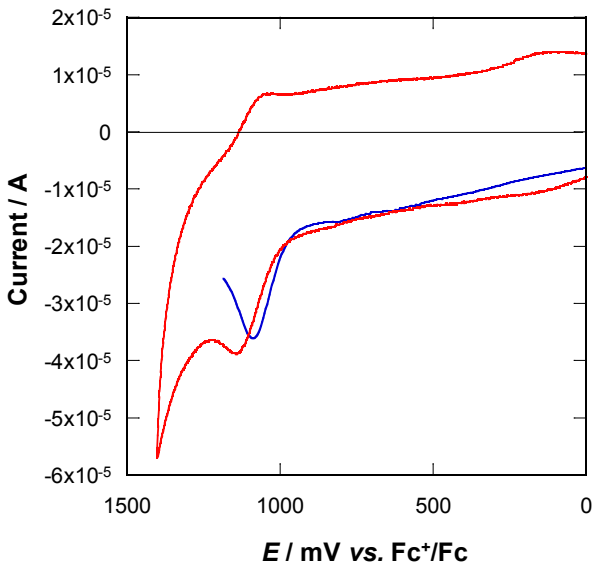

Figure S9. Cyclic (red) and OSW (blue) voltammograms of **Re**(pbn) (0.20 mM) under an Ar atmosphere. Voltammograms were taken at scan rates of 800 mV/s (CV) and 60 Hz (OSWV) in an acetonitrile solution with TBAH (0.1 M). A glassy carbon working electrode (area = 7.1 mm^2) was used.

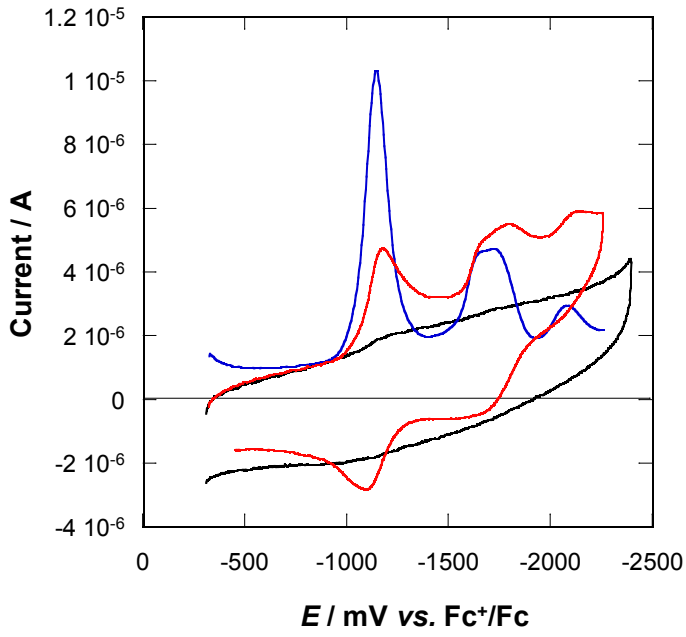

Figure S10. Cyclic (red) and OSW (blue) voltammograms of **Re**(pbn) (0.20 mM) and a blank (black) under an Ar atmosphere. Voltammograms were taken at scan rates of 100 mV/s (CV) and 15 Hz (OSWV) in an acetonitrile solution with TBAH (0.1 M). A glassy carbon working electrode (area = 7.1 mm^2) was used.

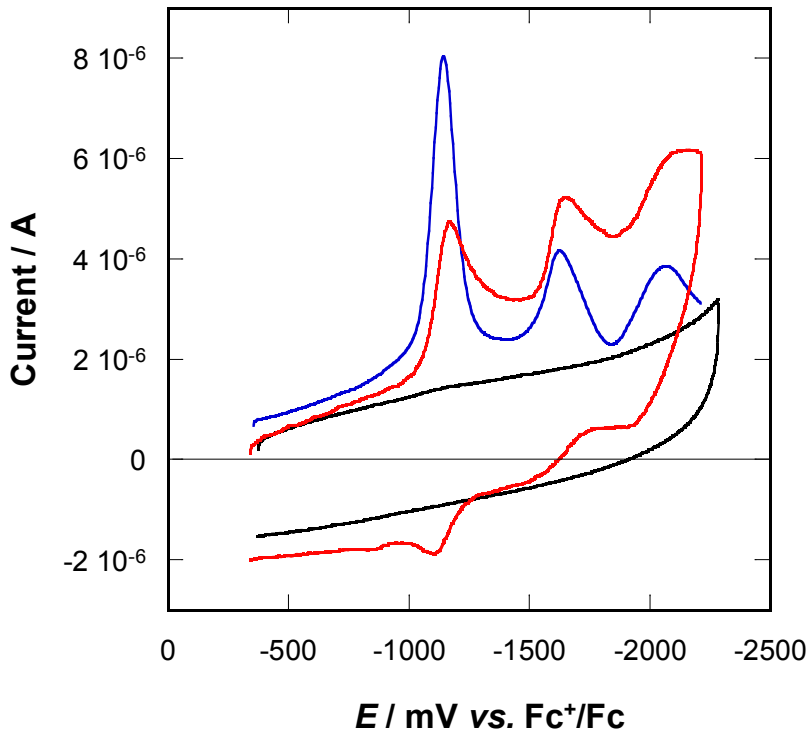

Figure S11. Cyclic (red) and OSW (blue) voltammograms of **Re**(pbn) (0.20 mM) and a blank (black) under an Ar atmosphere. Voltammograms were taken at scan rates of 100 mV/s (CV) and 15 Hz (OSWV) in an acetonitrile solution with TBAH (0.1 M) and water (~0.3 M). A glassy carbon working electrode (area = 7.1 mm^2) was used.

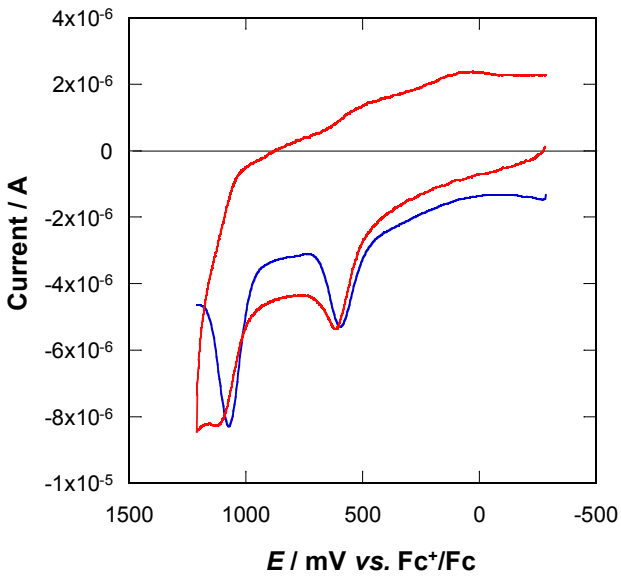

Figure S12. Cyclic (red) and OSW (blue) voltammograms of **Re**(pbnHH) (0.20 mM) under an Ar atmosphere. Voltammograms were taken at scan rates of 100 mV/s (CV) and 15 Hz (OSWV) in an acetonitrile solution with TBAH (0.1 M) and water (~0.3 M). A glassy carbon working electrode (area = 7.1 mm^2) was used.

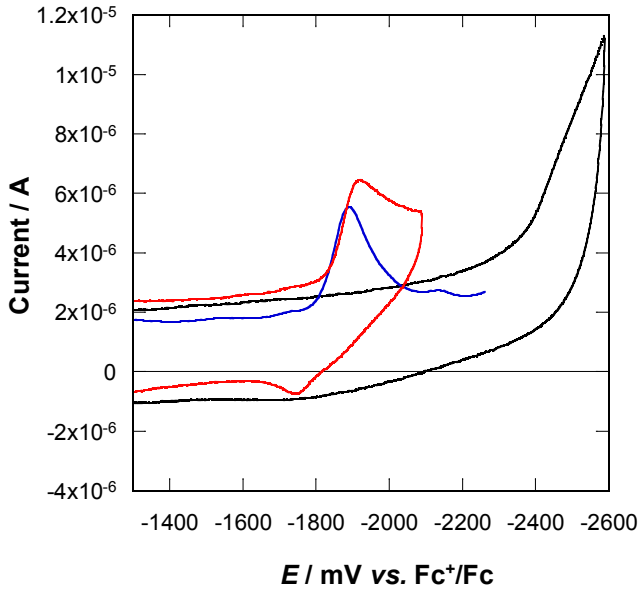

Figure S13. Cyclic (red) and OSW (blue) voltammograms of **Re**(pbnHH) (0.20 mM) and a blank (black) under an Ar atmosphere. Voltammograms were taken at scan rates of 100 mV/s (CV) and 15 Hz (OSWV) in an acetonitrile solution with TBAH (0.1 M) and water (~0.3 M). A glassy carbon electrode (area = 7.1 mm^2) was used as the working electrode.

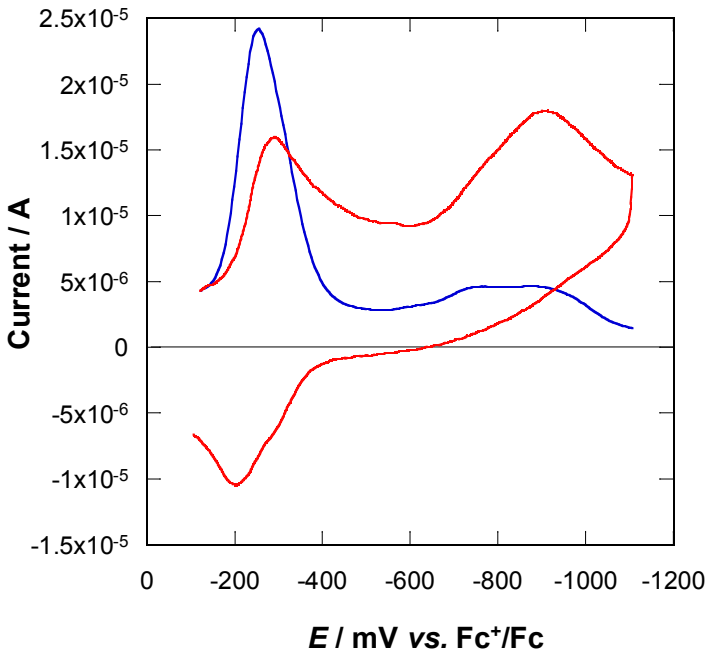

Figure S14. Cyclic (red) and OSW (blue) voltammograms of **Re**($pbnH^+$) (0.20 mM) under an Ar atmosphere. Voltammograms were taken at scan rates of 3.2 V/s (CV) and 120 Hz (OSWV) in an acetonitrile solution with TBAH (0.1 M) and HBF_4 (~2 mM). A stationary mercury drop (area ~ 1 mm^2) was used as the working electrode.

Na-Hg reduction of *fac*-[Re(pbn)(CO)$_3$Cl]

Spectral changes during Na-Hg reduction of **Re**(pbn) in acetonitrile are shown in Figure S15. Five absorption bands appeared at 339, 398, 540, 871 and 983nm, accompanied by the decay of absorption bands at 296 and 382 nm with clear isosbestic points during step-wise reduction. The resultant spectrum did not change for over 30 minutes. Similar NIR bands have been observed in the first reduction of Ru(bpy)$_2$(pbn)$^{2+}$ indicating that an electron is located in the benzonaphthyridine part of the pbn ligand.[10] Further reduction steps (from red to blue), which corresponds to the production of the doubly reduced species, changed the spectrum to one that possesses intense bands at 453 and 579 nm. The UV-vis spectrum acquired after double reduction is similar to that of *fac*-[Re(dmb)(CO)$_3$]$^-$ (dmb = 4,4'-dimethyl-2,2'-bipyridine).[11]

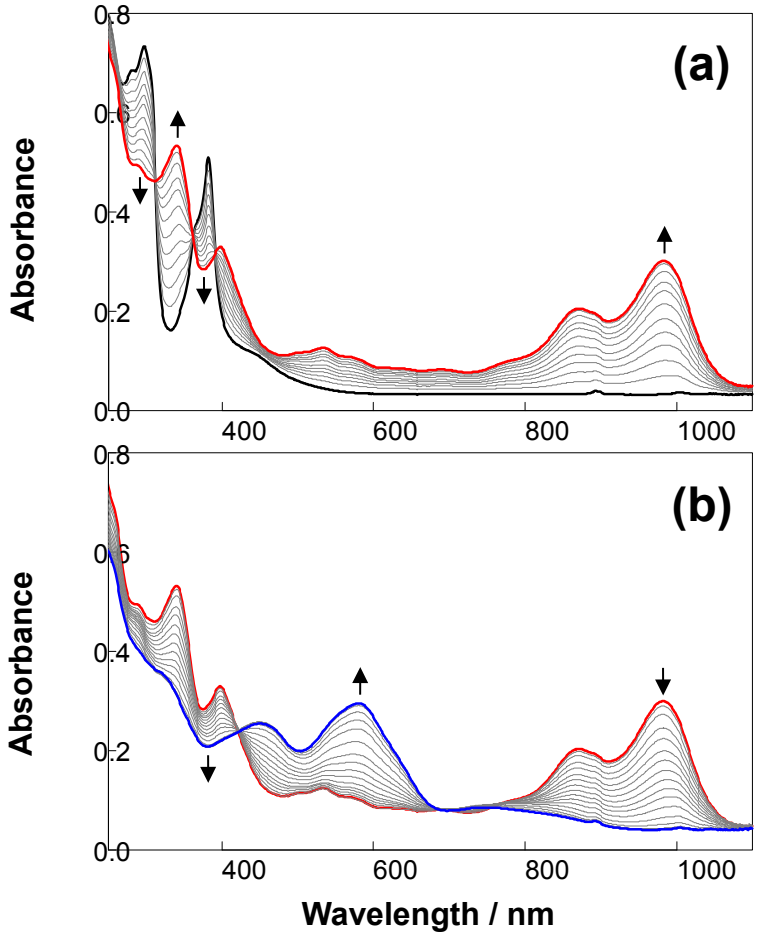

Figure S15. UV-vis absorption spectral changes during stepwise reduction of **Re**(pbn) by Na-Hg in a acetonitrile solution. (a) First and (b) second reduction steps are represented as transitions from the black (starting complex) to the red (1e-reduced) lines and from the red to the blue (doubly reduced) lines, respectively.

Nicholson-Shain plot for first reduction wave of *fac*-[Re(pbn)(CO)$_3$Cl] with or without water under an Ar atmosphere

In the CV of **Re**(pbn), the first reduction peak, which has a corresponding oxidation peak in the anodic scan, is reversible (Figure S10). Addition of water affects this first reduction process. As shown in the Nicholson plots (Figure S16), in the presence of water, certain chemical process(es) took place at low scanning rate, which is presumably assigned to the formation of **Re**(pbnHH) because it was previously found that the protonated one-electron-reduced complex $[Ru(bpy)_2(pbnH)]^{2+}$ disproportionated to give $[Ru(bpy)_2(pbn)]^{2+}$ and $[Ru(bpy)_2(pbnHH)]^{2+}$.[9] In fact, the reduction peak of **Re**(pbnHH) (see below) was observed in the cathodic scan only when the scan rate was below 100 mV/s.

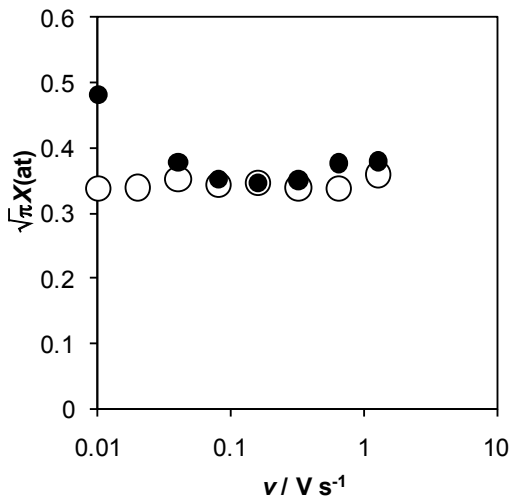

Figure S16. Nicholson-Shain plot of current functions of first reduction wave *vs.* scanning rate for a **Re**(pbn) acetonitrile solution without water (white) and with water (black) under an Ar atmosphere.

Voltammetry and controlled potential electrolysis under a CO_2 atmosphere

When the concentration of CO_2 dissolved in solution was varied by using nitrogen-CO_2 gas mixtures, a gradually increasing positive shift in the second reduction peak potential was observed with increasing CO_2 concentration as shown in Figure S18. This indicates that the second reduction process involves a chemical process, i.e., CO_2 binding to the complex because its Nicholson-Shain plot (Figure S17) has an upward slope with increasing scan rate in the region of high scanning rate (> 100 mV/s), suggesting that an E_rC_r-type mechanism, which is charge transfer to species O (E_r; eq. S1) followed by a reversible chemical reaction between species R and species Z (C_r; eq. S2), takes place.

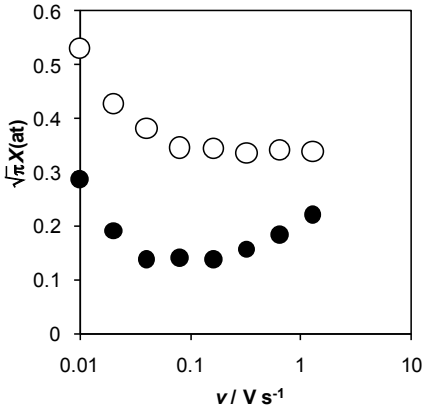

Figure S17. Nicholson-Shain plot of current functions of the first reduction wave (white) and second reduction wave (black) *vs.* scanning rate for a **Re**(pbn) acetonitrile solution containing water under CO_2 atmosphere.

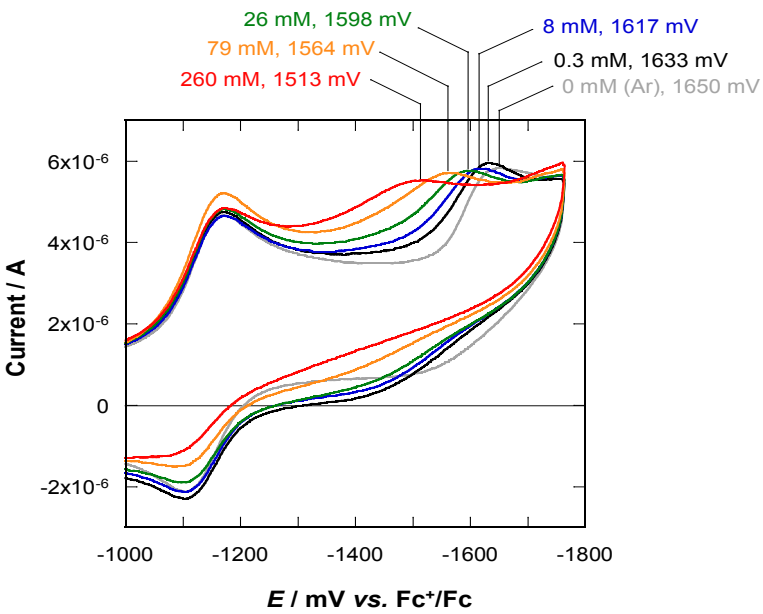

Figure S18. Peak potential shifts of the second reduction wave in CVs of 0.20 mM **Re**(pbn), 0.1 M TBAH and ~0.3 M water and 0 to 260 mM CO_2 in acetonitrile with scan rate of 100 mV/s.

Nicholson and Shain discussed the current function in the cathodic scan when a E_rC_r-type mechanism takes place. The peak shift is quantified by eq. S3 as developed from the current function they discussed.[7]

$$\mathrm{O} + \mathrm{e}^- \rightleftharpoons \mathrm{R} \tag{S1}$$

$$\mathrm{R} + \mathrm{CO_2} \underset{k_r}{\overset{k_f}{\rightleftharpoons}} \mathrm{Z} \tag{S2}$$

$$\frac{\Delta E_p}{RT/nF} = \frac{3}{2}\ln(1 + K[\mathrm{CO_2}]^q) + \frac{1}{2}\ln\frac{k_r}{v} - 2.41 \tag{S3}$$

In eq S3, K is an equilibrium constant of the following chemical process, ΔE_p is the shift, R is the ideal gas constant, T is the absolute temperature, F is Faraday's constant, n is the number of electrons involved in the catalytic reaction, q is the number of CO_2 molecules involved, v is scan rate, and k_f and k_r are the rate constants. A plot of peak potential shifts *vs.* $\ln(1 + K[CO_2]^q)$, was found to be linear when K is 40 M^{-1} and q is 1 (Figure S19). This plot indicates that the complex binds one CO_2 molecule during this E_rC_r-type process.

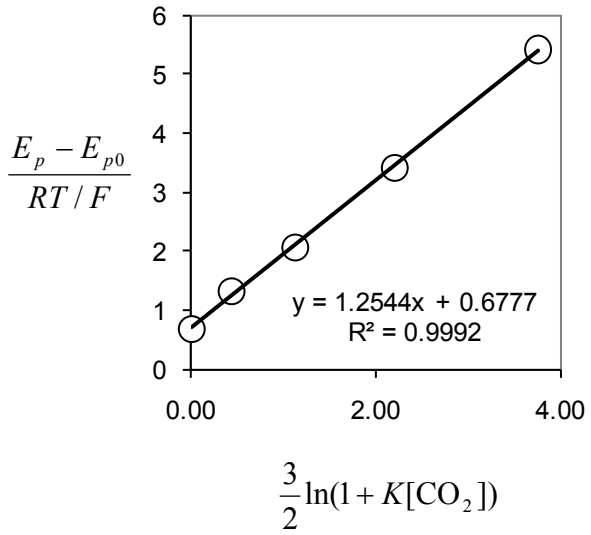

Figure S19. Plot of peak potential shifts *vs.* a function of $[CO_2]$. E_{p0} is the peak potential of the second reduction wave under an Ar atmosphere.

The variation of the concentration of CO_2 also affected the current enhancement observed at the third reduction peak potential under an Ar atmosphere. Nicholson and Shain discussed the current function in the cathodic scan when a E_rC'-type mechanism takes place, which is charge transfer to species O (E_r; eq. S4) followed by an irreversible chemical reaction of species R to regenerate species O (C'; eq. S5).[7] The ratio of peak current in the presence of CO_2 (i_c) to peak current in the absence of CO_2 (i_p) is quantified by eq. S6, as developed from the current function they discussed.

$$O + e^- \rightleftharpoons R \tag{S4}$$

$$R + CO_2 \xrightarrow{k_f} O + X \tag{S5}$$

$$\frac{i_c}{i_p} = \frac{n}{0.4463}\sqrt{\frac{RTk_f[CO_2]}{Fv}} = 0.72\sqrt{\frac{k_f[CO_2]}{v}} \tag{S6}$$

Since a plot of these currents *vs.* the square root of $[CO_2]$ was found to be linear, this suggests that the catalytic process involves one CO_2 (Figure S20) via an E_rC'-type mechanism. Using eq. S6, the k_f is estimated as 3×10^2 M^{-1} S^{-1}.

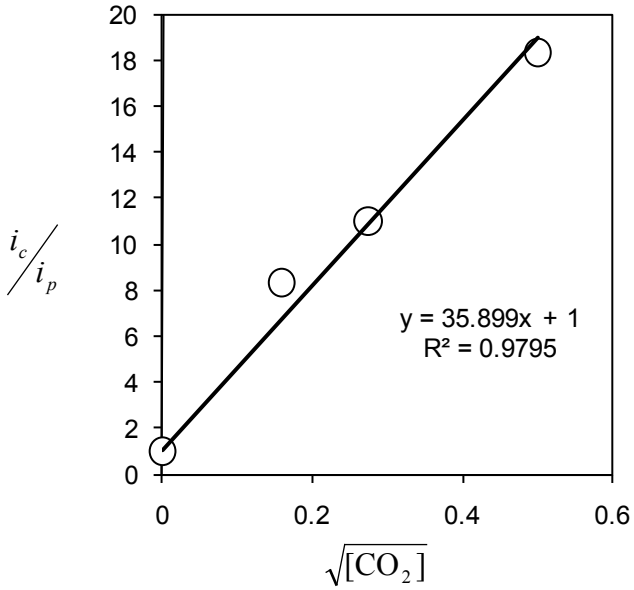

Figure S20. Plot of i_c/i_p *vs.* square root of $[CO_2]$.

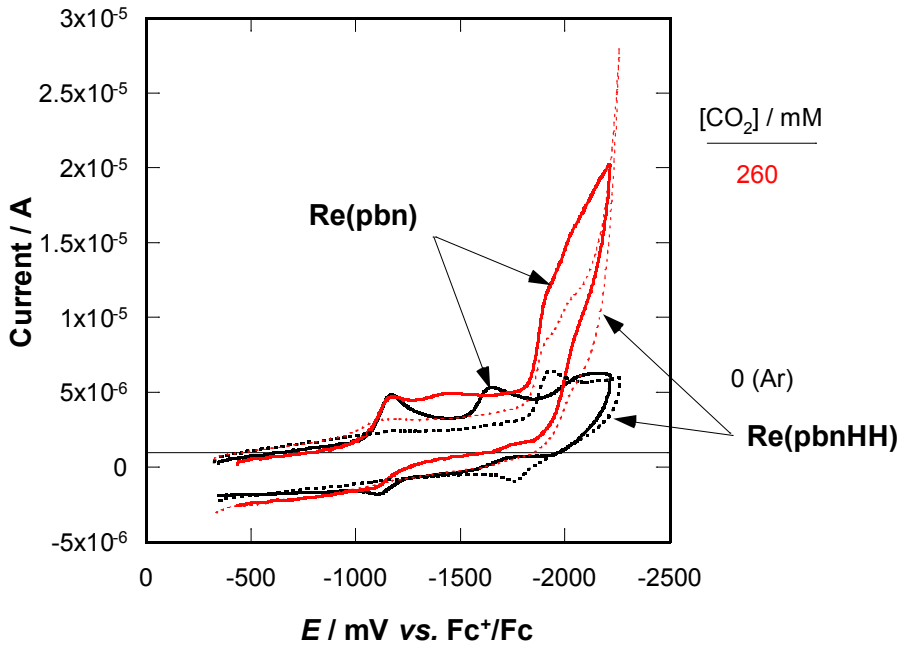

Figure S21. Cyclic voltammograms of **Re**(pbn) (solid line) and Re(pbnHH) (dotted line) under an Ar (black) and CO_2 (red) atmospheres.

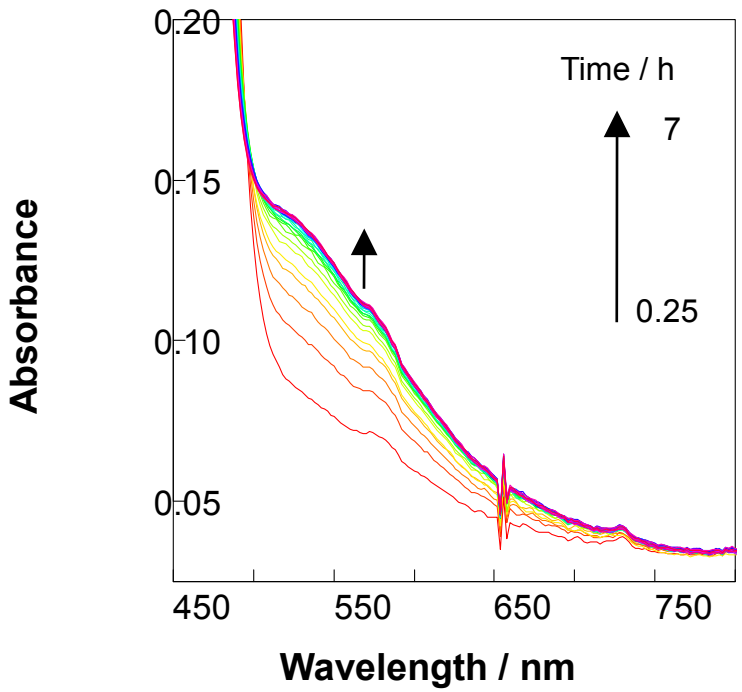

Figure S22. UV-vis absorption spectral changes of **Re**(pbnHH) (0.2 μmol) with $[Ph_3C]PF_6$ (0.2 μmol) in CH_3CN (0.7 mL) at room temperature.

References

1. K. Suzuki, A. Kobayashi, S. Kaneko, K. Takehira, T. Yoshihara, H. Ishida, Y. Shiina, S. Oishi and S. Tobita, *Phys. Chem. Chem. Phys.*, 2009, **11**, 9850-9860.
2. W. L. F. Armarego and C. L. L. Chai, *Purification of Laboratory Chemicals*, 5th edn., Elsevier, Oxford, U.K., 2003.
3. (a) A. Godard and G. Quéguiner, *J. Heterocycl. Chem.*, 1980, **17**, 465-473; (b) A. Godard and G. Quéguiner, *J. Heterocycl. Chem.*, 1982, **19**, 1289-1296; (c) T. Koizumi and K. Tanaka, *Angew. Chem. Int. Ed.*, 2005, **44**, 5891-5894.
4. K. C. Kurien, *J. Chem. Soc. B*, 1971, 2081-2082.
5. (a) J. Osteryoung and J. J. O'Dea, *Electroanal. Chem.*, 1986, **14**, 209; (b) M. J. Nuwer, J. J. O'Dea and J. Osteryoung, *Anal. Chim. Acta*, 1991, **251**, 13-25; (c) J. J. O'Dea, J. Osteryoung and R. A. Osteryoung, *Anal. Chem.*, 1981, **53**, 695-701; (d) J. J. O'Dea, K. Wikiel and J. Osteryoung, *J. Phys. Chem.*, 1990, **94**, 3628-3636.
6. V. M. Hultgren, A. W. A. Mariotti, A. M. Bond and A. G. Wedd, *Anal. Chem.*, 2002, **74**, 3151-3156.
7. R. S. Nicholson and I. Shain, *Anal. Chem.*, 1964, **36**, 706-723.
8. Y. Tomita, S. Teruya, O. Koga and Y. Hori, *J. Electrochem. Soc.*, 2000, **147**, 4164-4167.
9. T. Fukushima, E. Fujita, J. T. Muckerman, D. E. Polyansky, T. Wada, K. Tanaka, *Inorg. Chem.* 2009, **48**, 11510-11512.
10. D. E. Polyansky, D. Cabelli, J. T. Muckerman, T. Fukushima, K. Tanaka and E. Fujita, *Inorg. Chem.*, 2008, **47**, 3958-3968.
11. Y. Hayashi, S. Kita, B. S. Brunschwig and E. Fujita, *J. Am. Chem. Soc.*, 2003, **125**, 11976-11987.